

$2\nu_2 - \nu_1$. The far-field patterns of these three modes are shown in row *a* of Fig. 2. Similarly, along with mode 2, two "combination tones" can be generated having the same spatial field. Their far-field patterns are shown in row *b* of Fig. 2. Observation of the mode patterns of a gas laser in the presence of combination tones will thus yield combination patterns at four equidistant frequencies, as shown in row *c* of Fig. 2. This agrees with the experimental results of Haisma and Bouwhuis.²

It should be noted that the frequency difference between each pair of successive modes depends on the intensities of all modes concerned. Since there are three distances between the four modes, three conditions have to be fulfilled. A fourth condition determines the sum of the four intensities.

These four conditions can be met only for definite intensities of each of the four modes. These considerations will be of importance in any discussion of the mode intensity competition. Thus it may be that the combination tones cannot show up or that just one combination tone is observed.

Finally, we would remark that, for the occurrence of combination tones, it is essential that the two principal modes have different spatial distributions and that their frequency difference is close to the natural linewidth of the atomic transition.

¹H. G. van Bueren, J. Haisma, and H. de Lang, Phys. Letters **2**, 340 (1962).

²J. Haisma and G. Bouwhuis, Phys. Rev. Letters **12**, 287 (1964).

³W. E. Lamb, Jr., Phys. Rev. (to be published).

COMPARISON OF THE $^{16}\text{O}(p,t)$ AND $(p,^3\text{He})$ REACTIONS POPULATING ANALOG FINAL STATES IN ^{14}O AND $^{14}\text{N}^\dagger$

Joseph Cerny and Richard H. Pehl

Department of Chemistry and Lawrence Radiation Laboratory, University of California, Berkeley, California

(Received 4 May 1964)

Detailed comparative measurements of direct interaction transitions from an initial state to analog final states provide a sensitive experimental test of the charge independence of nuclear forces. Since few comparisons of direct transfer reactions to analog final states have been made and none under unambiguous direct reaction conditions, we have investigated the $^{16}\text{O}(p,t)^{14}\text{O}$ [g. s., 0^+ , $T=1$] and $^{16}\text{O}(p,^3\text{He})^{14}\text{N}$ [2.31 MeV, 0^+ , $T=1$] transitions induced by 43.7-MeV protons. Previous two-nucleon transfer investigations of the mass-14 isobaric triad have been reported utilizing the $^{12}\text{C}(^3\text{He},n)^{14}\text{O}$ (g. s.) and $^{12}\text{C}(^3\text{He},p)^{14}\text{N}$ (2.31 MeV) reactions at bombarding energies up to 2.6 MeV,¹ 1.8 to 5.5 MeV,² and 6 to 11 MeV.³ However, rigorous comparison of these low-energy measurements is handicapped by the relatively larger Coulomb effects and interference between the compound nucleus and direct reaction contributions to the transitions. A further difficulty arises in comparing the absolute cross sections since two different detecting systems must be employed.

The (p,t) and $(p,^3\text{He})$ measurements were induced by a beam of 43.7-MeV protons from the Berkeley 88-inch cyclotron. After energy analysis, the protons were brought into a 36-inch scatter-

ing chamber and impinged on a gas target. An improved particle identifier⁴ fed by a 40-mg/cm² dE/dx , 480-mg/cm² E semiconductor counter telescope distinguished the reaction products. A typical particle-identifier spectrum is shown in Fig. 1. Total energy pulses were fed into a Nuclear Data analyzer which was appropriately gated so that the triton and helium-3 spectra were recorded simultaneously, each spectrum in a 1024-channel group. The deuteron-triton valley and the entire α -particle spectrum of the identifier were also recorded in the analyzer to measure any small but possible loss of the t and ^3He groups in question. The average energy resolution was 190 keV for the tritons and 240 keV for the helium-3.

Figure 2 presents absolute cross-section measurements of the $^{16}\text{O}(p,t)^{14}\text{O}$ (g. s.) and $^{16}\text{O}(p,^3\text{He})^{14}\text{N}$ (2.31 MeV) transitions; the $(p,^3\text{He})$ differential cross sections have been multiplied by the theoretically required factor of 1.88 as will be discussed below. Representative statistics are shown on Fig. 2. Our independent absolute cross sections should be accurate to $\pm 10\%$; however, since the spectra were obtained simultaneously, the relative errors should be given primarily by the statistics. Although the differential cross sec-

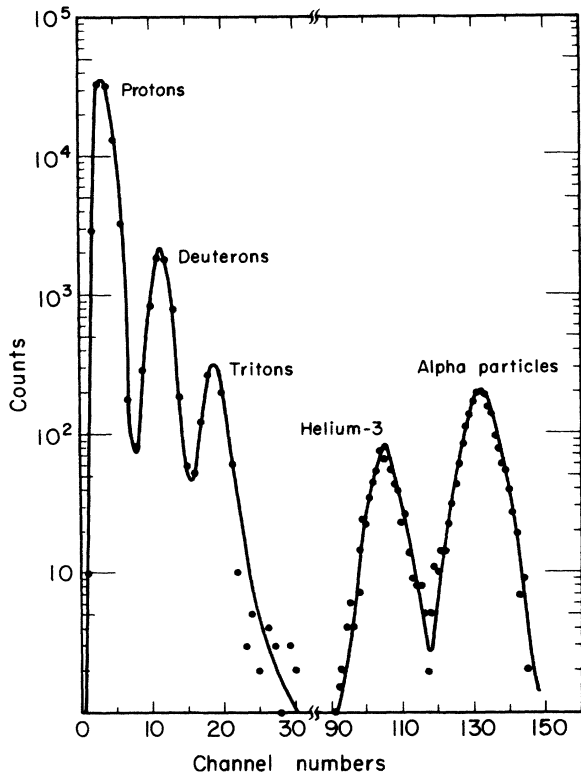


FIG. 1. Particle identifier spectrum from 43.7-MeV protons on ^{16}O .

tions vary by a factor of 100 over the angular range investigated, only slight departures from exact agreement are apparent.

In Born approximation, the ratio of these differential cross sections is given by

$$\frac{d\sigma(p,t)}{d\sigma(p,^3\text{He})} = \frac{k_t}{k_{^3\text{He}}} \frac{|M_t|^2}{|M_{^3\text{He}}|^2}$$

Assuming pure isospin states for all nuclei involved in the transitions and an isospin conserving interaction, the theoretical ratio of

$$\frac{|M_t|^2}{|M_{^3\text{He}}|^2} = \frac{C(t_p T_t; \tau_p, \tau_t - \tau_p)^2}{C(t_p T_{^3\text{He}}; \tau_p, \tau_{^3\text{He}} - \tau_p)^2} = 2$$

(T is the isospin of the transferred pair). Since the ratio of $k_t/k_{^3\text{He}}$ is 0.94, the (p,t) reaction should be favored by a factor of 1.88 over the $(p,^3\text{He})$ reaction.

The above calculation has also ignored the effects of the differing energies and Coulomb scattering in the exit channels, and an indication of this is of interest. Glendenning has performed a preliminary calculation of these $0^+ \rightarrow 0^+$, $L=0$

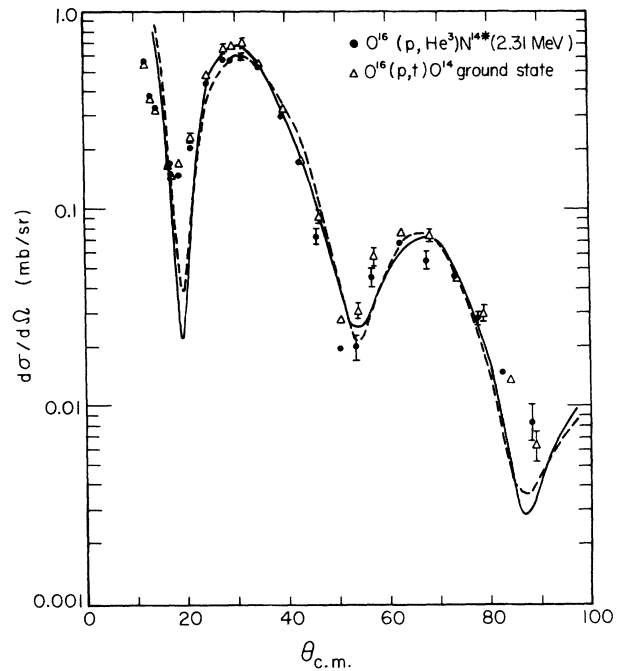


FIG. 2. Angular distributions for the $^{16}\text{O}(p,t)^{14}\text{O}[g.s., 0^+, T=1]$ and $^{16}\text{O}(p,^3\text{He})^{14}\text{N}[2.31 \text{ MeV}, 0^+, T=1]$ transitions; the latter cross sections have been multiplied by 1.88. The solid and dashed lines are $L=0$, two-nucleon transfer DWBA fits to the (p,t) and $(p,^3\text{He})$ transitions, respectively. The optical-model parameters for these fits were

	V	W	a	b	r_0	r_1
p	-55	-12	0.6	0.6	1.3	0
t and ^3He	-60	-20	0.5	0.5	1.3	1.2

transitions using his two-nucleon transfer, distorted-wave Born approximation (DWBA) code.⁵ The fits are also shown in Fig. 2. Identical optical-model potentials were used in the incident and exit channels (no isospin-dependent term was included), and both calculations required a cutoff radius of 5.2 F; the nucleons were assumed to be picked up from the $p_{1/2}$ shell. Since at present these theoretical calculations do not give absolute cross sections, the two curves were normalized to each other at 0° and the $^{16}\text{O}(p,t)^{14}\text{O}(g.s.)$ fit was normalized to the experimental data at the 30° peak.

The theoretical angular distributions shown in Fig. 2 fit the data very well. It can be seen that a reduction of the $^{16}\text{O}(p,^3\text{He})^{14}\text{N}(2.31 \text{ MeV})$ cross section relative to the $^{16}\text{O}(p,t)^{14}\text{O}(g.s.)$ cross section at the 30° peak is predicted in accord with the experimental results; the fits at the 65° peak agree with the data within our statistics.

Further calculation shows that the variation at the 30° peak arises primarily from the difference in energy of the outgoing particles.

The ratio of the integrated cross sections (11- 90° c. m.) for these transitions, after correcting for the phase-space and isospin coupling factors, is $\sigma(p, t)/\sigma(p, {}^3\text{He}) = 0.905 \text{ mb}/0.807 \text{ mb} = 1.12/1$. This excellent agreement between the absolute cross sections, and the angular distributions, implies a strongly charge-independent interaction operator. Further, the analog states of ${}^{14}\text{O}$ and ${}^{14}\text{N}$ must be extremely similar. In addition to the principal $[(p_{1/2})^2]0^+$, $T=1$ component in these states, there can be admixtures of 0^+ states of $T \neq 1$ and admixtures of other 0^+ , $T=1$ states. Since these amplitudes enter linearly into the matrix elements, though appropriately weighted by transition-dependent factors, the matrix-element ratio is a sensitive measure of differing amplitude and phase admixtures in the analog states.

Exact comparison of the ${}^{14}\text{O}$ (g. s.) and ${}^{14}\text{N}$ (2.31 MeV) wave functions must await an accurate calculation of the effect of the different energies and Coulomb scattering in the exit channels on the relative cross sections. For example, however, let us assume that the ratio of the matrix elements depends solely upon differences in the wave functions of the analog states of ${}^{14}\text{O}$ and ${}^{14}\text{N}$. Also,

we will assume that this difference arises only from a unique $T=0$ impurity in the ${}^{14}\text{N}$ (2.31 MeV) state⁶ of 2×10^{-3} with a single amplitude and phase of -0.045 . The predicted ratio of $\sigma(p, t)/\sigma(p, {}^3\text{He})$ would then be 1.10/1, which is comparable to the experimental ratio, even though the admixture is quite small.

We are indebted to Dr. Norman K. Glendenning for many valuable discussions.

[†]Work performed under the auspices of the U. S. Atomic Energy Commission.

¹D. A. Bromley, E. Almqvist, H. E. Gove, A. E. Litherland, E. B. Paul, and A. J. Ferguson, Phys. Rev. **105**, 957 (1957).

²G. V. Din, H. M. Kuan, and T. W. Bonner, Nucl. Phys. **50**, 267 (1964).

³H. W. Fulbright, W. Parker Alford, O. M. Bilaniuk, V. K. Deshpande, and J. W. Verba, University of Rochester Report No. NYO-10034, 5 February 1962 (unpublished).

⁴F. S. Goulding, D. A. Landis, J. Cerny, and R. H. Pehl (to be published).

⁵N. K. Glendenning (private communication). A detailed description of these calculations will be published.

⁶W. M. Macdonald, *Nuclear Spectroscopy*, edited by F. Ajzenberg-Selove (Academic Press, Inc., New York, 1960), Pt. B, p. 932.

ANALYSIS OF THE 1.0- TO 1.4-BeV π - ρ ENHANCEMENT*

Suh Urk Chung, Orin I. Dahl, Lyndon M. Hardy, Richard I. Hess, George R. Kalbfleisch, Janos Kirz, Donald H. Miller, and Gerald A. Smith

Department of Physics and Lawrence Radiation Laboratory, University of California, Berkeley, California
(Received 20 April 1964)

Peripheral interactions of 8- to 16-BeV/c π mesons in heavy-liquid bubble chambers have been studied by Bellini *et al.*¹ and Huson and Fretter.² Both groups observed significant enhancements in the $\pi^-\pi^+\pi^-$ effective-mass distributions in the 1.0- to 1.4-BeV region; however, it was not possible to determine whether the effect resulted from the production of a new resonant state or from kinematics of diffraction dissociation. Recently, in a thorough analysis of the reaction $\pi^+ + p \rightarrow \pi^+ + \pi^+ + \pi^- + p$ at 3.65 BeV/c, Goldhaber *et al.* showed that most events could be classified into two distinct groups, $\rho^0 N^{*++}(1238)$ and $\rho^0 \pi^+ p$.³ They observed the 1.0- to 1.4-BeV enhancement only in the $\rho^0 \pi^+ p$ events. We have studied this strong π - ρ interaction in $\pi^- + p \rightarrow \pi^+ + \pi^- + \pi^- + p$ and find that the enhance-

ment consists of two clearly resolved peaks. In addition, decay of the higher mass system into $K\bar{K}$ is observed in the $K\bar{K}N$ final states. Possible spin and parity assignments for the two states are discussed.

The film was obtained in the course of a systematic study of 1.5- to 4.2-BeV/c $\pi^- p$ interactions in the Lawrence Radiation Laboratory's 72-in. hydrogen bubble chamber. Approximately 30 000 pictures at 3.22 BeV/c with an average of 10 pions each were scanned for interactions leading to four charged secondaries; 7500 events were measured and processed. Where possible, ambiguities were removed by comparison of track ionization on the film with that calculated from the kinematic fits. For the remainder of the events, the fit with the highest confidence level